AD750496

551.63
G1372

~~Vose~~

FTD-MT-24-2156-71

FOREIGN TECHNOLOGY DIVISION

FOUR-LEVEL METHOD FOR PREDICTING GEOPOTENTIAL IN THE TROPOSHPERE AND LOWER STRATOSPHERE TAKING RADIATION AND TURBULENT HEAT TRANSFER INTO CONSIDERATION

by

M. B. Galin, A. K. Popov and S. I. Rudenko

STATE WATER SURVEY DIVISION
LIBRARY COPY

~~MAR 18 1974~~

APR 01 1974

Approved for public release;
distribution unlimited.

ILLINOIS STATE WATER SURVEY LIBRARY COPY

DATE DUE

551.63
G1372
07110407

Galin, M.B.
FOUR-LEVEL METHOD
FOR PREDICTING
GEOPOTENTIAL IN THE
TROPOSPHERE AND
LOWER STRATOSPHERE

DEMCO

551.65
G1372

FTD-MT- 24-2156-71

EDITED MACHINE TRANSLATION

FTD-MT-24-2156-71

FOUR-LEVEL METHOD FOR PREDICTING GEOPOTENTIAL IN THE TROPOSHPERE AND LOWER STRATOSPHERE TAKING RADIATION AND TURBULENT HEAT TRANSFER INTO CONSIDERATION

By: M. B. Galin, A. K. Popov and S. I. Rudenko

English pages: 17

Source: Voprosy Gidrodinamicheskoy Teorii Klimata i Dolgosrochnogo Prognoza Pogody (Questions Concerning the Hydrodynamic Theory of Climate and Long-Term Weather Forecasting), No. 12, 1966, pp. 21-34.

Requester : FTD/PTR

This document is a SYSTRAN machine aided translation, post-edited for technical accuracy by: Alc Paul J. Reiff Jr.

STATE WATER SURVEY DIVISION
LIBRARY COPY
APR 01 1974

Approved for public release;
distribution unlimited.

THIS TRANSLATION IS A RENDITION OF THE ORIGINAL FOREIGN TEXT WITHOUT ANY ANALYTICAL OR EDITORIAL COMMENT. STATEMENTS OR THEORIES ADVOCATED OR IMPLIED ARE THOSE OF THE SOURCE AND DO NOT NECESSARILY REFLECT THE POSITION OR OPINION OF THE FOREIGN TECHNOLOGY DIVISION.	PREPARED BY: TRANSLATION DIVISION FOREIGN TECHNOLOGY DIVISION WP-AFB, OHIO.

FTD-MT- 24-2156-71 **Date** 28 July **19** 72

Digitized by the Internet Archive
in 2023 with funding from
University of Illinois Urbana-Champaign Alternates

https://archive.org/details/fourlevelmethodf00gali

U. S. BOARD ON GEOGRAPHIC NAMES TRANSLITERATION SYSTEM

Block	Italic	Transliteration	Block	Italic	Transliteration
А а	*А а*	A, a	Р р	*Р р*	R, r
Б б	*Б б*	B, b	С с	*С с*	S, s
В в	*В в*	V, v	Т т	*Т т*	T, t
Г г	*Г г*	G, g	У у	*У у*	U, u
Д д	*Д д*	D, d	Ф ф	*Ф ф*	F, f
Е е	*Е е*	Ye, ye; E, e*	Х х	*Х х*	Kh, kh
Ж ж	*Ж ж*	Zh, zh	Ц ц	*Ц ц*	Ts, ts
З з	*З з*	Z, z	Ч ч	*Ч ч*	Ch, ch
И и	*И и*	I, i	Ш ш	*Ш ш*	Sh, sh
Й й	*Й й*	Y, y	Щ щ	*Щ щ*	Shch, shch
К к	*К к*	K, k	Ъ ъ	*Ъ ъ*	"
Л л	*Л л*	L, l	Ы ы	*Ы ы*	Y, y
М м	*М м*	M, m	Ь ь	*Ь ь*	'
Н н	*Н н*	N, n	Э э	*Э э*	E, e
О о	*О о*	O, o	Ю ю	*Ю ю*	Yu, yu
П п	*П п*	P, p	Я я	*Я я*	Ya, ya

* ye initially, after vowels, and after ъ, ь; e elsewhere. When written as ё in Russian, transliterate as yë or ë. The use of diacritical marks is preferred, but such marks may be omitted when expediency dictates.

FOLLOWING ARE THE CORRESPONDING RUSSIAN AND ENGLISH DESIGNATIONS OF THE TRIGONOMETRIC FUNCTIONS

Russian	English
sin	sin
cos	cos
tg	tan
ctg	cot
sec	sec
cosec	csc
sh	sinh
ch	cosh
th	tanh
cth	coth
sch	sech
csch	csch
arc sin	sin^{-1}
arc cos	cos^{-1}
arc tg	tan^{-1}
arc ctg	cot^{-1}
arc sec	sec^{-1}
arc cosec	csc^{-1}
arc sh	sinh^{-1}
arc ch	cosh^{-1}
arc th	tanh^{-1}
arc cth	coth^{-1}
arc sch	sech^{-1}
arc csch	csch^{-1}

rot	curl
lg	log

FOUR-LEVEL METHOD FOR PREDICTING GEOPOTENTIAL IN THE TROPOSHPERE AND LOWER STRATOSPHERE TAKING RADIATION AND TURBULENT HEAT TRANSFER INTO CONSIDERATION

M. B. Galin, A. K. Popov and S. I. Rudenko

The linear four-level scheme for predicting geopotential at isobaric surfaces at the 50, 150, 250, and 950 mb for the earth's northern hemisphere is used. A computational method is proposed and examples are given for predicting (geopotential) for up to three days.

In the present work, a four-level model of baroclinic atmosphere is used for predicting geopotential. To calculate the inflow of heat from radiation and turbulent heat transfer we use the method set forth in [1]. As our initial equations, we take the equation of vortex transfer and the equation of the inflow of heat in quasi-solenoidial approximation [2]:

$$\frac{\partial \Delta\psi}{\partial t} + \frac{1}{a^2 \sin\theta}(\psi,\ \Delta\psi + 2\omega a^2 \cos\theta) = -2\omega a^2 \cos\theta \frac{\partial W}{\partial \xi}, \qquad (1)$$

$$\frac{\partial T'}{\partial t} + \frac{1}{a^2 \sin\theta}(\psi,\ T') + \frac{RT_{cp}}{g}(\gamma_a - \gamma)\frac{W}{\xi} = F, \qquad (2)$$

where ψ is the flow function, T' - is deviation of temperature from standard distribution, $\tilde{\rho}(z)$ and $\tilde{P}(z)$ - are standard distributions of density and pressure, $\xi = \tilde{P}(z)/\tilde{P}(0)$, v_z - is vertical velocity

$$W=\frac{g}{RT_{\text{cp}}}\,\xi v_z=\frac{g\widetilde{\rho}\ (z)}{\widetilde{P}\,(0)},$$

F is expressed thus, [1]:

$$F=\frac{1}{N}\left[\frac{2}{m^2-1}\frac{\partial^2 T'}{\partial\zeta^2}-2T'+e^{-\zeta}\int\limits_0^{\zeta}T'e^{\zeta}\,d\zeta+\right.$$
$$\left.+e^{\zeta}\int\limits_{\zeta}^{Z}T'e^{-\zeta}\,d\zeta+\mu e^{\zeta-Z}T'_Z\left(\frac{dT}{dE}\right)_{\text{cp}}\right], \qquad (3)$$

where $\zeta=\int\limits_z^{\infty}\alpha_2\rho_w\,dz$ is optical thickness; ρ_W - is the density of the substance which absorbs the radiation; α_2 - is the coefficient of absorption of long-wave radiation: $\mu=4r\sigma T^3_Z$; λ' - is the coefficient of turbulent heat transfer in a vertical direction; σ - is the Stephan-Boltzman constant; c_p - is the heat capacity of the air under constant pressure; $Z=(\zeta)_{z=0}$;

$$N=\left(\frac{c_p\widetilde{\rho}}{\alpha_2\rho_w}\frac{dT}{dE}\right)_{\text{cp}},$$
$$\frac{2}{m^2-1}=\left(\lambda'\alpha_2\rho_w\frac{dT}{dE}\right)_{\text{cp}}.$$

We linearize equations (1) and (2) with respect to the zone flow, for which we present the functions in the following form:

$$\psi=-a^2\alpha(\xi)\cos\theta+\psi'',$$
$$T'=T_0+M(\xi)\sin^2\theta+T'',$$
$$F=\overline{F}+F^{\cdot},$$

where ψ", T" and F" - are nonstationary nonzonal parts.

From the relationship between the zonal parts of the functions of flow and temperature, $\overline{T}=-\frac{\xi}{R}2\omega\cos\theta\frac{\partial\overline{\psi}}{\partial\xi}$, comes the relation between parameter M and the index circulation α.

$$M=-\frac{2\omega}{R}a^2\xi\frac{d\alpha}{d\xi}.$$

After linearization we obtain:

$$\left(\frac{\partial}{\partial t}+\alpha\frac{\partial}{\partial\lambda}\right)\Delta\psi''+2(\alpha+\omega)\frac{\partial\psi''}{\partial\lambda}=-2\omega a^2\cos\theta\frac{\partial W}{\partial\xi}; \qquad (4)$$

$$\left(\frac{\partial}{\partial t}+\alpha\frac{\partial}{\partial\lambda}\right)T''-\frac{2M}{a^2}\cos\theta\,\frac{\partial\psi''}{\partial\lambda}+\frac{RT_{cp}}{g}\,\frac{(\gamma_a-\gamma)\,W}{\xi}=F''. \tag{5}$$

As a boundary condition vertically we take

$$W(0)=W(1)=0.$$

We proceed in equations (4) and (5) to the finite differences vertically. For this, we analyze the entire thickness of the atmosphere with respect to variable ξ in 20 equal parts (such that $\Delta\xi = 0.05$) by points ξ, ξ_2, ..., ξ_{19}. Further, we write the equation of vortex transfer (4) for the four levels: ξ_1, ξ_3, ξ_5, ξ_{19}, where $\xi_1 = 0.05$; $\xi_3 = 0.15$, $\xi_5 = 0.25$ and $\xi_{19} = 0.95$. The equation for the inflow of heat (5) is written for three levels: ξ_2, ξ_4, ξ_{12}, where $\xi_2 = 0.1$, $\xi_4 = 0.2$, $\xi_{12} = 0.6$. Substituting for the derivatives ratios of finite differences, after several transformations we obtain four equations for vortex transfer and three equations for the inflow of heat. Further, we use the condition of quasi-geostrophism and the barometric formula for replacing T". The derived equations are transferred according to (3). Finally we will get:

$$\begin{aligned}&\left(\frac{\partial}{\partial t}+\alpha_1\frac{\partial}{\partial\lambda}\right)\left[\Delta\psi_1''+\gamma\left(\psi_3''-\psi_1''\right)\right]+\beta_{1,0}\frac{\partial\psi_1''}{\partial\lambda}-\\&-\beta_{1,3}\frac{\partial}{\partial\lambda}\left(\psi_1''+\psi_3''\right)+\alpha_{1,3}\left(\psi_3''-\psi_1''\right)-\alpha_{1,5}\left(\psi_5''-\psi_3''\right)=0;\end{aligned} \tag{6}$$

$$\begin{aligned}&\left(\frac{\partial}{\partial t}+\alpha_3\frac{\partial}{\partial\lambda}\right)\left[\Delta\psi_3''-\gamma\left(\psi_3''-\psi_1''\right)+4\gamma\left(\psi_5''-\psi_3''\right)\right]+\\&+\beta_{3,0}\frac{\partial\psi_3''}{\partial\lambda}-\beta_{3,5}\frac{\partial}{\partial\lambda}\left(\psi_3''+\psi_5''\right)-\beta_{3,1}\frac{\partial}{\partial\lambda}\left(\psi_1''+\psi_3''\right)-\alpha_{3,1}\left(\psi_3''-\psi_1''\right)+\\&+\alpha_{3,5}\left(\psi_5''-\psi_3''\right)=0;\end{aligned} \tag{7}$$

$$\begin{aligned}&\left(\frac{\partial}{\partial t}+\alpha_5\frac{\partial}{\partial\lambda}\right)\left[\Delta\psi_5''-\gamma\left(\psi_5''-\psi_3''\right)+1{,}25\left(\psi_{19}''-\psi_5''\right)\right]+\\&+\beta_{5,0}\frac{\partial\psi_5''}{\partial\lambda}-\beta_{5,3}\frac{\partial}{\partial\lambda}\left(\psi_3''+\psi_5''\right)-\beta_{5,19}\frac{\partial}{\partial\lambda}\left(\psi_5''+\psi_{19}''\right)+\alpha_{5,1}\left(\psi_3''-\psi_1''\right)-\\&-\alpha_{5,3}\left(\psi_5''-\psi_3''\right)=0;\end{aligned} \tag{8}$$

$$\begin{aligned}&\left(\frac{\partial}{\partial t}+\alpha_{19}\frac{\partial}{\partial\lambda}\right)\left[\Delta\psi_{19}''-1{,}25\gamma\left(\psi_{19}''-\psi_5''\right)\right]+\beta_{19,0}\frac{\partial\psi_{19}''}{\partial\lambda}-\\&-\beta_{19,5}\frac{\partial}{\partial\lambda}\left(\psi_5''+\psi_{19}''\right)=0,\end{aligned} \tag{9}$$

where

$$\frac{1}{\gamma}=\Gamma=\frac{R^2T_{\text{cp}}}{4\omega^2a^2g}\left(\frac{\gamma_a-\gamma}{\cos^2\theta}\right)_{\text{cp}};$$

$$\beta_{1,0}=2(\alpha_1+\omega)-\frac{1}{\Gamma}(\alpha_3-\alpha_1),\quad \beta_{1,3}=-\beta_{3,1}=\frac{\alpha_3-\alpha_1}{2\Gamma};$$

$$\alpha_{1,3}=\frac{26{,}1}{N\Gamma};\quad \alpha_{1,5}=\frac{7{,}4}{N\Gamma};$$

$$\beta_{3,0}=2(\alpha_3+\omega)+\frac{1}{\Gamma}(\alpha_3-\alpha_1)-\frac{4}{\Gamma}(\alpha_5-\alpha_3);$$

$$\beta_{3,5}=\frac{2(\alpha_5-\alpha_3)}{\Gamma};$$

$$\alpha_{3,1}=\frac{41{,}7}{N\Gamma};\quad \alpha_{3,5}=\frac{29{,}0}{N\Gamma};$$

$$\beta_{5,0}=2(\alpha_5+\omega)+\frac{1}{\Gamma}(\alpha_5-\alpha_3)-\frac{1{,}25}{\Gamma}(\alpha_{19}-\alpha_5);$$

$$\beta_{5,3}=\frac{\alpha_3-\alpha_5}{2\Gamma};\quad \beta_{5,19}=-\beta_{19,5}=\frac{0{,}62(\alpha_{19}-\alpha_5)}{\Gamma};$$

$$\alpha_{5,1}=\frac{3{,}9}{N\Gamma};\quad \alpha_{5,3}=\frac{5{,}4}{N\Gamma};$$

$$\beta_{19,0}=2(\alpha_{19}+\omega)+\frac{1{,}25}{\Gamma}(\alpha_{19}-\alpha_5).$$

We search for the solution of the system (6)-(9) in the form

$$\psi_k=C_k e^{-im(\lambda+\sigma^m t)}P_n^m(\cos\theta),\quad k=1,\ 3,\ 5,\ 19. \tag{10}$$

To define the constant C_k we get a system of four algebraic equations. This system has a nontrivial solution if the determinant for the unknowns equals zero, from which the characteristic equation for the determination of σ^m is obtained. C_k and σ^m are, generally speaking, complex, that is $C_k=A_k+iB_k$, $\sigma^m=\sigma_r+i\sigma_i$.

The system indicated above of four algebraic equations permits the expression of the constants C_k for various levels by means of the analogous constants of any one level. In this instance we accepted the level corresponding to k = 5, which leads to the following relationships:

$$\begin{gathered}A_k=k_{rk}A_5-k_{ik}B_5,\\ B_k=k_{rk}B_5+k_{ik}A_5,\\ k=1,\ 3,\ 19,\end{gathered} \tag{11}$$

where k_{rk} and k_{ik} are constants, defining σ_r and σ_i. Since for each n and m we have four values for σ, then in place of relationships (11) we in fact have four relationships. Finally the solution takes the form:

$$\psi_k' = \sum_{m=1}^{18} \sum_{n=m}^{36} (M_{kn}^m \cos m\lambda + N_{kn}^m \sin m\lambda)\, P_n^m(\cos\theta), \tag{12}$$

where

$$\begin{aligned} M_{kn}^m = \Big[& (A_k^1 \cos m\sigma_r^1 t + B_k^1 \sin m\sigma_r^1 t)\, e^{m\sigma_i^1 t} + (A_k^2 \cos m\sigma_r^2 t + \\ & + B_k^2 \sin m\sigma_r^2 t)\, e^{m\sigma_i^2 t} + (A_k^3 \cos m\sigma_r^3 t + B_k^3 \sin m\sigma_r^3 t)\, e^{m\sigma_i^3 t} + \\ & + (A_k^4 \cos m\sigma_r^4 t + B_k^4 \sin m\sigma_r^4 t)\, e^{m\sigma_i^4 t} \Big]_n^m, \\ N_{kn}^m = \Big[& (B_k^1 \cos m\sigma_r^1 t - A_k^1 \sin m\sigma_r^1 t)\, e^{m\sigma_i^1 t} + (B_k^2 \cos m\sigma_r^2 t - \\ & - A_k^2 \sin m\sigma_r^2 t)\, e^{m\sigma_i^2 t} + (B_k^3 \cos m\sigma_r^3 t - A_k^3 \sin m\sigma_r^3 t)\, e^{m\sigma_i^3 t} + \\ & + (B_k^4 \cos m\sigma_r^4 t - A_k^4 \sin m\sigma_r^4 t)\, e^{m\sigma_i^4 t} \Big]_n^m, \\ & k = 1,\ 3,\ 5,\ 19. \end{aligned} \tag{13}$$

To determine A_k and B_k we use the initial conditions:

$$\psi_k'^{0} = \sum_{m=1}^{18} \sum_{n=m}^{36} (A_k^0 \cos m\lambda + B_k^0 \sin m\lambda)\, P_n^m(\cos\theta), \quad k = 1,\ 3,\ 5,\ 19. \tag{14}$$

The sums on the right sides of (12) and (14) contain the terms corresponding to the even differences n - m.

If in relationships (13) we assume t = 0 and use (11) and (14), we obtain for a determination of A_5 and B_5 a system of equations of the eighth order, with coefficients which will be numbers k_{rk} and k_{ik}, but which in the right sides will have A_k^0 and B_k^0 for k = 1, 3, 5, 19.

We accomplish the transfer to geopotential using the relationship $\psi_k = \frac{g}{l_{cp}} H_k$, where l_{cp} - is the mean value of the Coriolis parameter.

Computation is carried out according to the following scheme. We determine the initial expansion factors A_k^0 and B_k^0, the mean-zonal values and circulation indexes α_1, α_3, α_5, α_{19}, according to the initial geopotential fields. The standard functions - Legendre's polynomials $P_n^m(\cos\theta)$ are considered each time and programmed in the machine's memory. Knowing the circulation indexes, we find the coefficients of the characteristic equation, and then σ. According to the values of σ and A_k^0, B_k^0 we find A_5, B_5 by means of the solution of the eight-order system. Further, with the help of (11) we determine A_k and B_k for $k = 1, 3, 19$, while we find M_{kn}^m and N_{kn}^m for any moment in time t according to formula (13). Summarizing series (12), we compute the desired values for the forecast fields.

The initial fields of the altitudes of the isobaric surfaces 150 and 250 mb were obtained by means of interpolation of the data of standard levels. Meanwhile it was assumed that the relationship between the altitudes of the isobaric surfaces were the same as for standard atmosphere. The altitudes of the isobaric surface 950 mb were obtained at sea level pressure with the assistance of a barometric step, for which a value of 8.5 m/mb was accepted. In this way we used the following formulas:

$$\begin{aligned} H_{150} &= 0{,}414H_{100} + 0{,}586H_{200}, \\ H_{250} &= 0{,}456H_{200} + 0{,}544H_{300}, \\ H_{950} &= 0{,}85\,(p_0 - 950). \end{aligned}$$

Since p_0 is the sea level pressure in millibars, then for H_{950} we must get values in decimeters. After forecast H_{50}, H_{150}, H_{250} and H_{950} is computed, we can recalculate the forecast values at standard levels according to formulas which are obtained similarly to (15):

$$\begin{aligned} H_{100} &= 0{,}371H_{50} + 0{,}629H_{150}, \\ H_{200} &= 0{,}437H_{150} + 0{,}563H_{250}, \\ H_{300} &= H_{250} - 120, \\ p_0 &= 950 + 1{,}176H_{950}. \end{aligned}$$

The problem was programmed for calculation by an electronic computer. The forecast was computed for several days with the values for the geopotential of isobaric surfaces for each day printed. The calculation of the forecast for a 24 hour period for all four surfaces took about 10 minutes. A whole series of examples was calculated, from which we reproduce two; one relates to the winter season (1 Feb 64), while the second relates to the summer (15 July 64). Zonal circulation in these two instances was substantially different. Thus, for 1 Feb. 1964 the zonal velocity monotonically increases with height, which is evident from the values of the circulation indexes: $\alpha_{19}/\omega = 0.012$; $\alpha_5/\omega = 0.067$; $\alpha_3/\omega = 0.072$; $\alpha_1/\omega = 0.087$. For 15 July 1964 the circulation has a different nature. At high altitudes, beginning at the 50 mb level, we find an easterly zonal flow which is a general characteristic of the summer season. The circulation indexes in this case take on the values: $\alpha_{19}/\omega = 0.002$; $\alpha_5/\omega = 0.047$; $\alpha_3/\omega = 0.039$; $\alpha_1/\omega = 0.009$.

We examine the forecast according to the initial data for 1 Feb. 1964 (0300, Moscow time). A comparison of the forecast charts AT_{50} for 1, 2, 3 day periods with the actual charts for that period shows that, as a whole, the synoptic situation was grasped by the forecast correctly. On the forecast chart for 2 Feb. 1964 (the first 24 hours of the forecast) it is possible to notice a high pressure center over the Pyrenean Peninsula. On the actual map, a ridge corresponds to this center. The position of troughs over Asia Minor, the Himalayas, and the Pacific Ocean were correctly given. In the second 24 hour period, high and low pressure centers over Central Europe and the Mediterranean respectively were forecast accurately. In the third 24 hour period (Figures 1, 2) on the actual chart we see the weakening of the designated centers which is insufficiently reflected in the forecast. We examine the forecast charts AT_{200} for the first 24 hour period. The position of troughs over the European territory of the USSR and the Atlantic is correctly forecast. The ridge over the Urals was satisfactorily obtained, although with a slight displacement

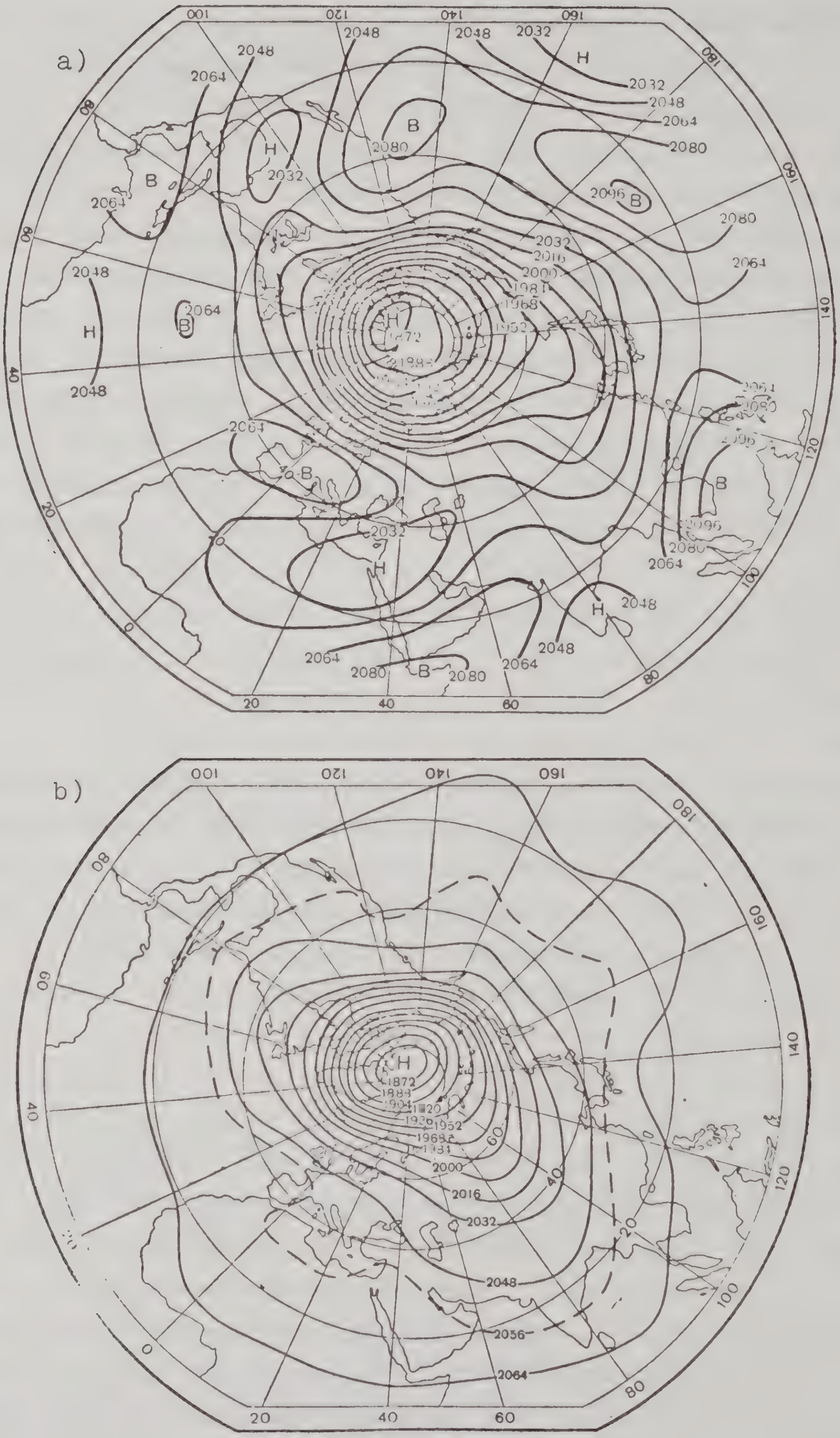

Fig. 1. Chart AT_{50}, 0300 Moscow time, 4 Feb 1964, a) forecast (3 day); b) actual.

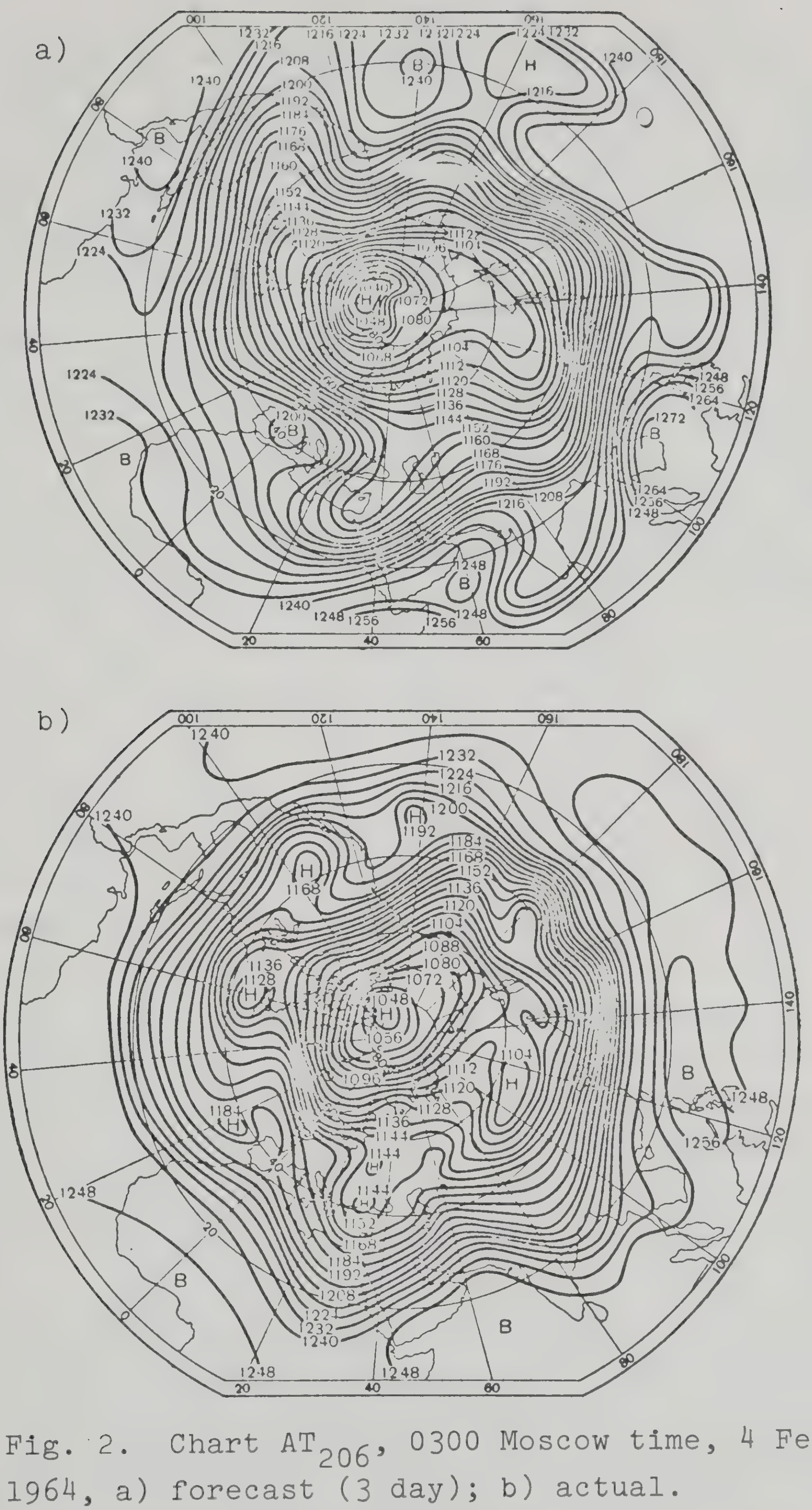

Fig. 2. Chart AT_{206}, 0300 Moscow time, 4 Feb 1964, a) forecast (3 day); b) actual.

to the east. In Siberia, a low pressure in the region of Krasnoyarsk was correctly obtained. In the second 24 hour period, the troughs over the European territory of the USSR and a ridge over West Europe were also correctly forecast. The coincidence of forecast with the actual in the area of the Atlantic and the USA should be noted. In the third 24 hour period (Fig. 2) an area of low pressure over Siberia is displaced to the east on the forecast chart in comparison to its actual position. The situation over North America appears smoother than it actually was. The forecast chart of isobaric surface 950 mb was compared with the basis of the surface pressure field. In the first 24 hour period (Fig. 3), low pressure centers over Scandinavia, pressure centers over the eastern portion of the Mediterranean Sea, to the east of Japan, over the USA, including in the region of the Aleutian Islands, were forecast. In subsequent periods, centers over the west coast of the USA, Japan, Scandinavia, and Siberia were satisfactorily obtained. The center over the Pyrenean was displaced to the east and exaggerated in comparison to the actual center. During the third 24 hour period, the forecast chart shows a high pressure region over the Pyrenean Peninsula, a low pressure region over the eastern portion of the Mediterranean Sea, and a vast high pressure area over Central Asia. All these areas coincide well with the analogous barometric formations on the actual chart. At the same time, two high pressure regions appear over the Pacific Ocean instead of the single one which appears on the actual map. The intense low in the region of the Labrador Peninsula appears weaker and is displaced to the west.

We now examine an example of forecasting according to the source data for 15 July 1964. On the first 24 hour period, the formation of low pressure center at isobaric surface 50 mb is forecast on the ridge over the Atlantic, just as the formation of a high pressure center over the European territory of the USSR. The zonal circulation in the middle latitudes corresponds with the actual situation over the USA. In the second 24 hour period a high pressure center was discovered over Europe. The low

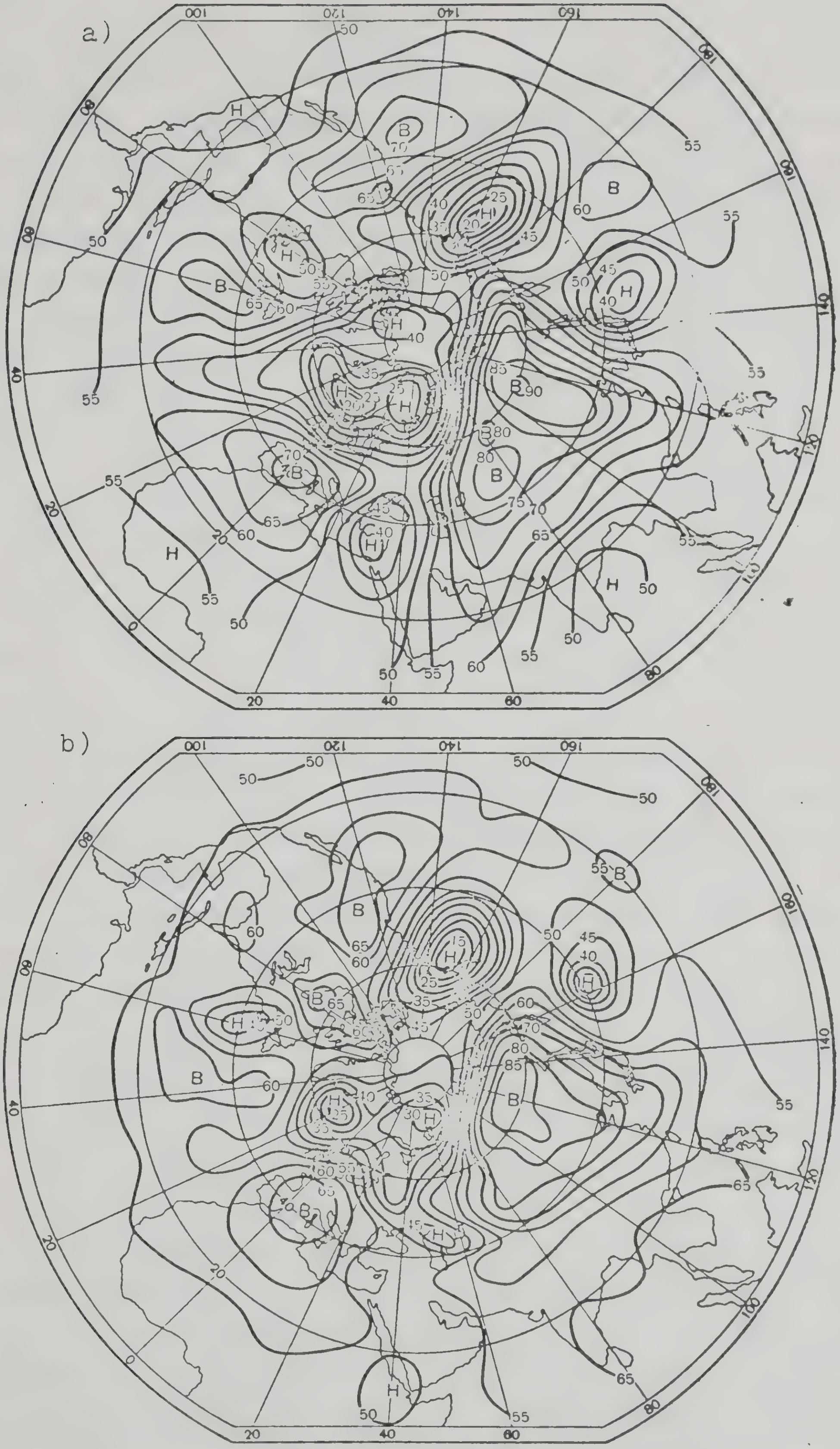

Fig. 3. Chart AT_{950}, 0300 Moscow time, 2 Feb 1964, a) forecast (3 day); b) actual.

pressure centers over the Himalayas and Atlantic and the high pressure center over the Caspaian were exaggerated. In the third 24 hour period, (Fig. 4) the low pressure center over the northern coast of Canada and a high pressure region over the USA and Scandinavia were forecast. On the 200 mb surface, high pressure centers were forecast over China, Arabia, Mexico; low pressure centers over the Okhotsk Sea, and troughs over the Atlantic and a ridge over the European territory of the USSR were also forecast. In the second 24 hour period the situation over Siberia, the far east of the USSR, and the USA was correctly depicted. The location of troughs over the Atlantic, the Black Sea, Central Asia, and Canada was satisfactorily predicted. In the third 24 hour period (Fig. 5) the situation in the middle latitudes was forecast better (the trough in the region of Greenland, the ridge over the northern European territory of the USSR, the trough over eastern Siberia and in the region of the west coast of the USA). The pressure centers in the southern latitudes appeared displaced to the east in comparison to their actual location. In the first 24 hour period on the 950 mb surface high pressure centers over Central Europe, the Atlantic Ocean, the western-most Pyrenean Peninsula, southern coast of the USA, north of Alaska and over the Pacific Ocean, and low pressure centers over Arabia, Tibet, eastern Siberia, and the west coast of the USA, (Fig. 6) were forecast. In the second 24 hour period, the meridional flow over Central Europe and the southwest flow over northwest Europe were forecast, as was the case in the first 24 hour period. The situation over the eastern USA and the Pacific Ocean coincide with the actual. Cyclonic formations over Tibet, south of Greenland and over the Pacific Ocean east of Japan were reported. In the third 24 hour period (Fig. 7) a low pressure center over the Pacific Ocean was accurately forecast. At the same time, a low pressure belt, coming across the Asian continent, was split into two intensive centers on the forecast chart. The same applied to the high pressure region over the Atlantic. The high pressure region over Western Siberia appeared displaced to the northwest.

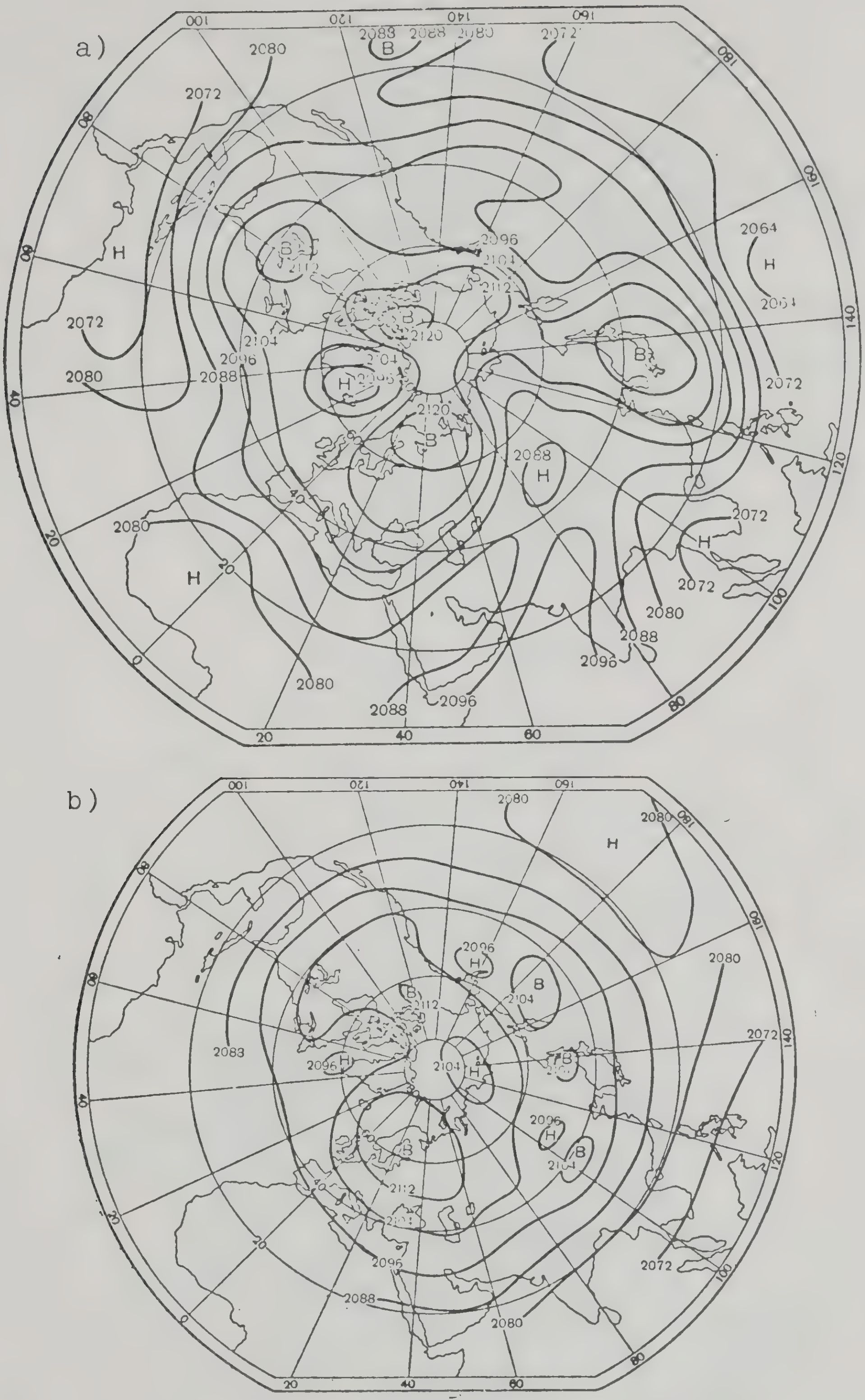

Fig. 4. Chart AT_{50}, 0300 Moscow time, 18 July 1964, a) forecast (3 day); b) actual.

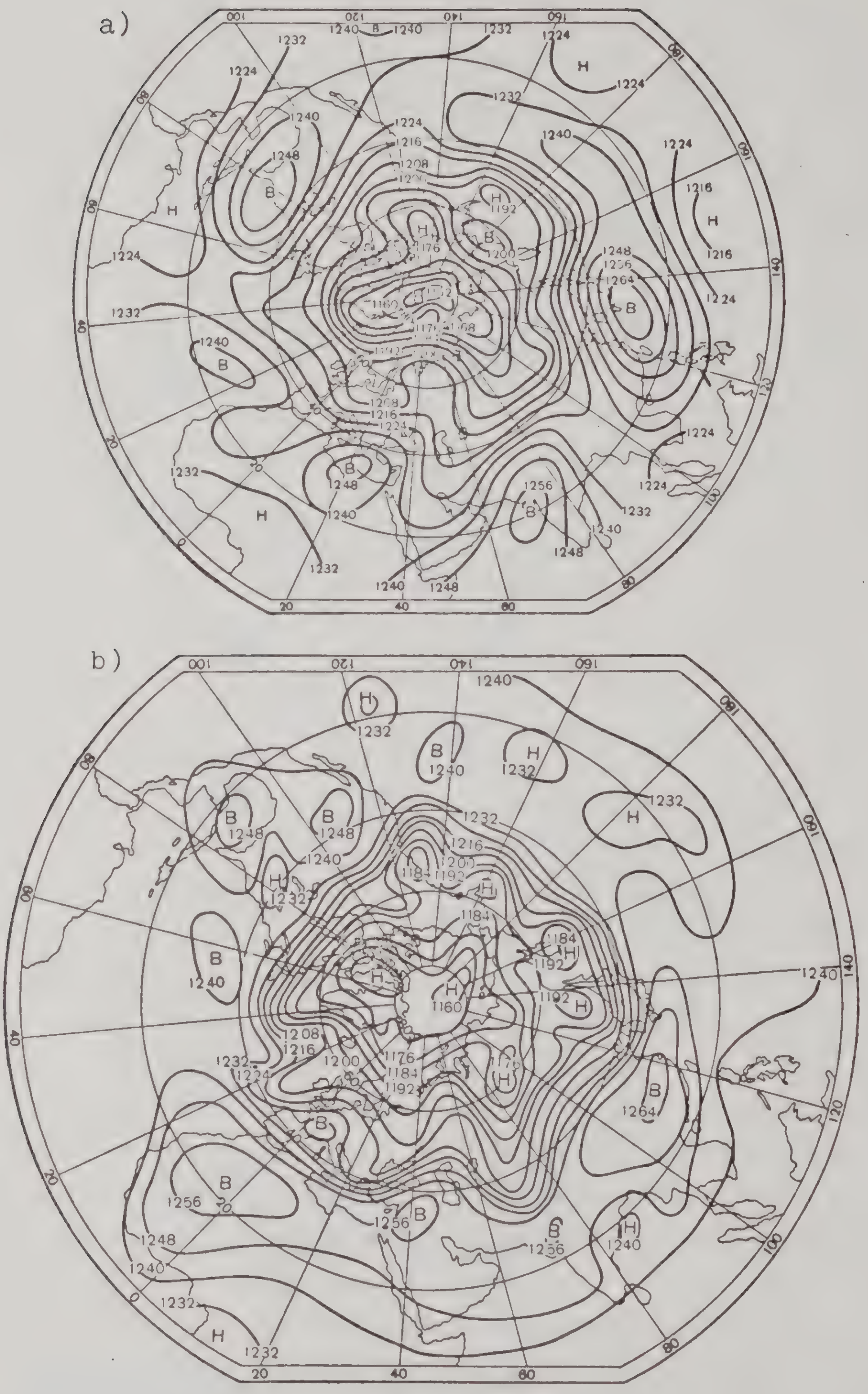

Fig. 5. Chart AT_{200}, 0300 Moscow time, 18 July 1964, a) forecast (3 day); b) actual.

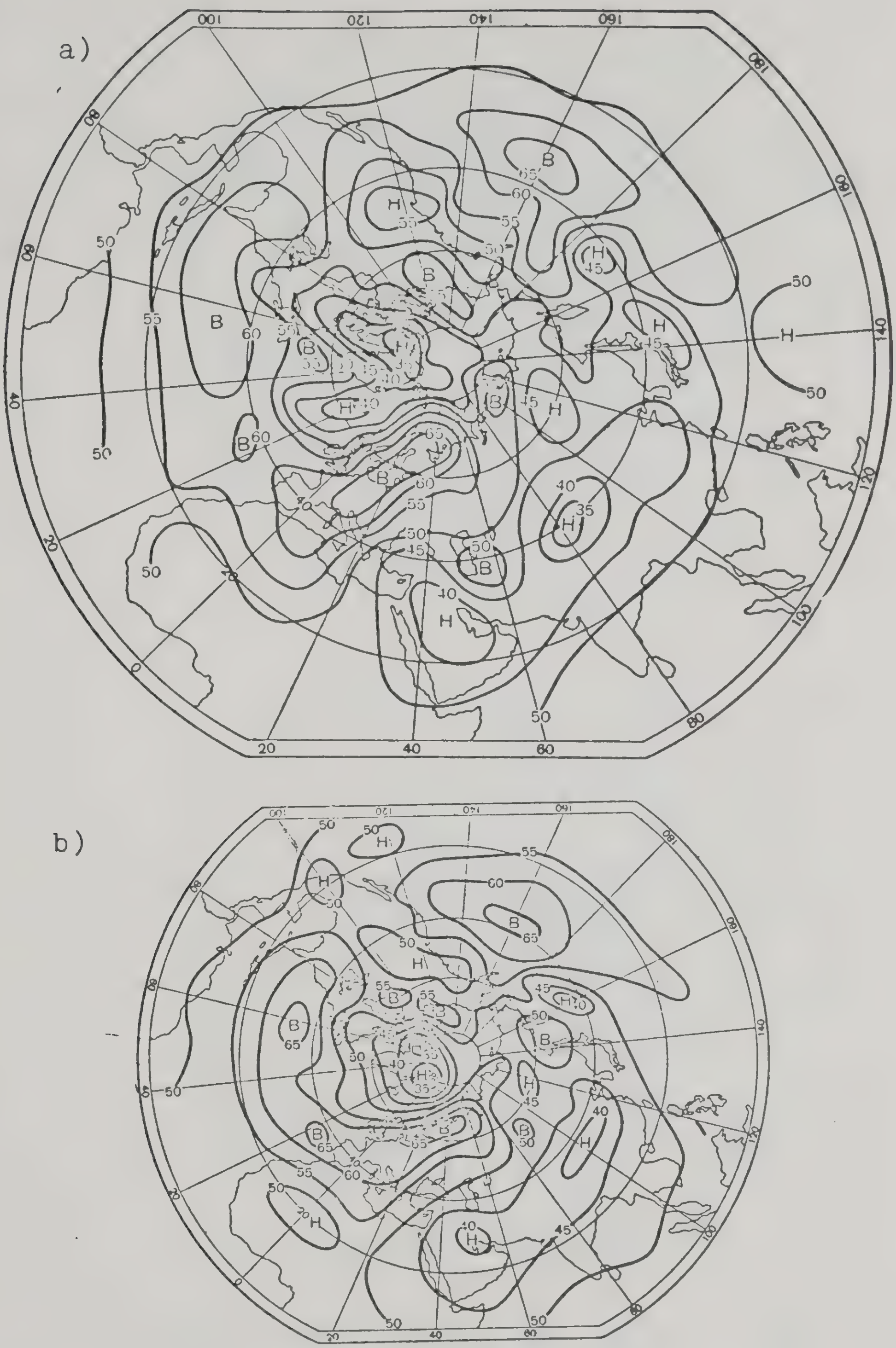

Fig. 6. Chart AT$_{950}$, 0300 Moscow time, 16 July 1964, a) forecast (3 day); b) actual.

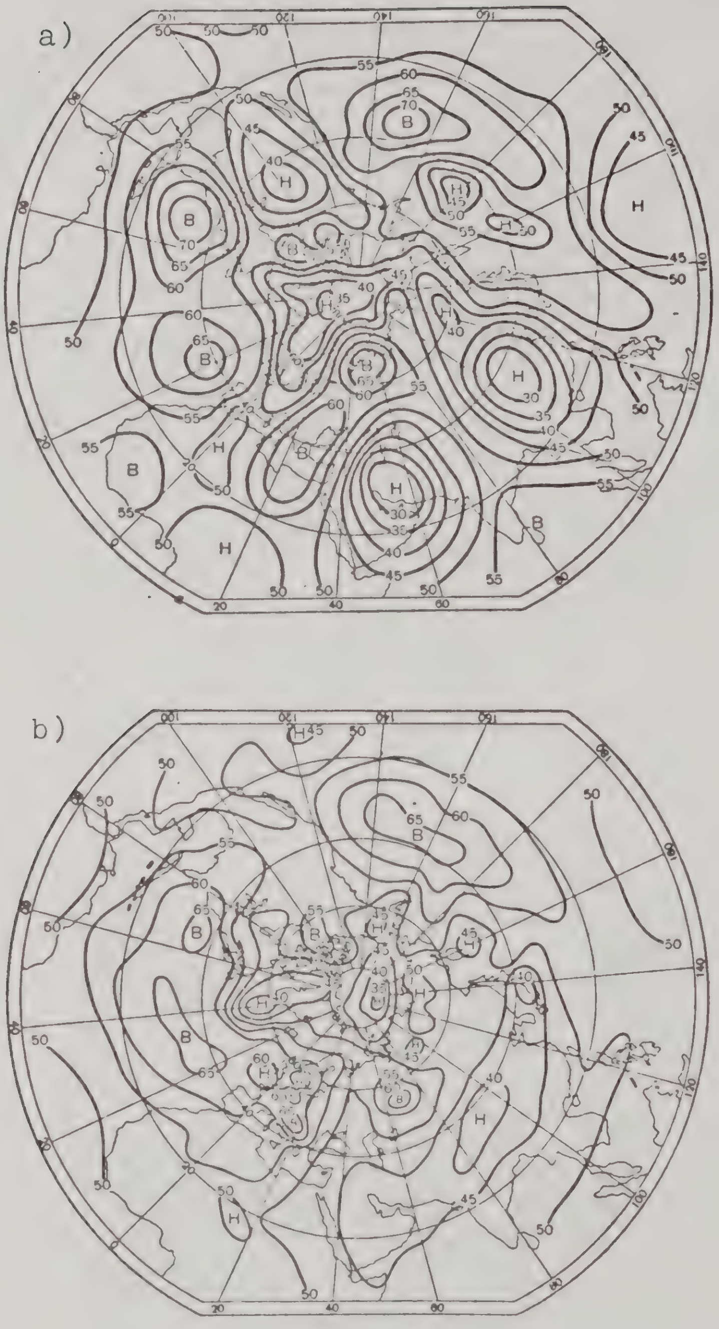

Fig. 7. Chart AT$_{950}$, 0300 Moscow time, 18 July 1964, a) forecast (3 day); b) actual.

Bibliography

1. **Блинова** Е. Н. К гидродинамической теории климата и долгосрочного прогноза погоды. Сб. «Гидродинамический долгосрочный прогноз погоды». Изд-во «Наука», М., 1964.
2. **Блинова** Е. Н. Метод решения нелинейной задачи об атмосферных движениях планетарного масштаба. ДАН СССР, т. III, № 6, 1956.
3. **Галин** М. Б. Гидродинамический прогноз метеорологических элементов в тропосферы и нижней стратосфере с учетом излучения и турбулентной теплопроводности. Тр. ММЦ, вып. 5, 1965.

DOCUMENT CONTROL DATA - R & D

(Security classification of title, body of abstract and indexing annotation must be entered when the overall report is classified)

1. ORIGINATING ACTIVITY *(Corporate author)* Foreign Technology Division Air Force Systems Command U. S. Air Force	2a. REPORT SECURITY CLASSIFICATION UNCLASSIFIED 2b. GROUP

3. REPORT TITLE

FOUR-LEVEL METHOD FOR PREDICTING GEOPOTENTIAL IN THE TROPOSHPERE AND LOWER STRATOSPHERE TAKING RADIATION AND TURBULENT HEAT TRANSFER INTO CONSIDERATION

4. DESCRIPTIVE NOTES *(Type of report and inclusive dates)*

Translation

5. AUTHOR(S) *(First name, middle initial, last name)*

M. B. Galin, A. K. Popov and S. I. Rudenko

6. REPORT DATE	7a. TOTAL NO. OF PAGES	7b. NO. OF REFS
1966	17	3

8a. CONTRACT OR GRANT NO. b. PROJECT NO. 60103 c. d.	9a. ORIGINATOR'S REPORT NUMBER(S) FTD-MT-24-2156-71 9b. OTHER REPORT NO(S) *(Any other numbers that may be assigned this report)*

10. DISTRIBUTION STATEMENT

Approved for public release; distribution unlimited.

11. SUPPLEMENTARY NOTES	12. SPONSORING MILITARY ACTIVITY Foreign Technology Division Wright-Patterson AFB, Ohio

13. ABSTRACT

A four-level model of a baroclinic atmosphere is used to predict geopotential at isobaric surfaces at the 50, 150, 250, and 950 millibar levels for the Northern Hemisphere. An outline for use in making the calculations is presented, and examples of predictions for periods up to 3 days are included. The problem was programmed for an electronic computer. Machine time involved in predictions for all four levels for one 24-hour period is approximately 10 minutes.

Security Classification

14. KEY WORDS	LINK A		LINK B		LINK C	
	ROLE	WT	ROLE	WT	ROLE	WT
Troposphere						
Stratosphere						
Atmospheric Geopotential						
Thermal Radiation						
Heat Conductivity						
Atmospheric Turbulence						
Turbulent Heat Transfer						
Weather Forecasting						
Computer Application						
Computer Programming						
Meteorology						

UNCLASSIFIED

Security Classification

DISTRIBUTION LIST

Organization		Nr. Cys.
AIR FORCE		
E053	AF/INAKA	1
E017	AF/RDGC - AFSC	1
E018	AF/RDGC - SAMSO	1
	ARL/CA	2
E404	AEDC	1
E408	AFWL	1
E410	ADTC	1
E413	ESD	2
	AFCRL (CRTE)	(1)
E427	RADC	1
E429	SAMSO	1
	FTD	
	LNA	1
	CCN	1
	NIA/PHS	2
	NIIR	10
	NIT	1
	PDT/PHE	15
	PDYA	1
	WE	1

Organization		Nr. Cys.
DISTRIBUTION DIRECT TO RECIPIENT		
	DDC	12
A205	DMATC	1
A210	DMAAC/PDA	2
B344	DIA/DS-4C	5
C043	SURG GEN	1
C509	ABERDEEN R & D CTR	1
C513	PICATINNY ARSENAL	1
C523	HARRY DIAMOND LAB	1
C535	AVIATION SYS COMD	1
C557	USAIIC	1
C591	FSTC	7
C619	MIA REDSTONE	1
D008	NAVSTIC	1
D217	NAVWPNSCEN	1
D220	CNR	1
H300	USAICE (USAREUR)	1
P055	CIA/CRS/ADD/SD	5
OTHER GOVERNMENT AGENCIES		
AEC (Wash)		2
FAA		1
NASA (ATSS-T)		1

UNIVERSITY OF ILLINOIS-URBANA
3 0112 112968703